



STUDIES ON THE ANTIBACTERIAL ACTIVITY OF GREEN SYNTHESIZED SILVER NANOPARTICLES

***Jai Shanker Pillai HP**

Department of Microbiology, Faculty of Science, Assam downtown University, Guwahati, Assam, India, *Email: drjaishankerpillai@gmail.com

Justin M Farook

Institute of Medicine, Yerevan Haybusak University, Yerevan, Armenia.
Email: justinfarook@gmail.com

Challaraj Emmanuel E.S

Department of Life Sciences, Kristu Jayanti College (Autonomous), K. Narayanapura, Kothanur Post, Bengaluru, Karnataka, India, Email: challaraj.e@kristujayanti.com

Chandrakala Linganna

Department of Environmental Science, Gulbarga University, Kalaburagi, Karnataka, India.
Email: ckala.lk@gmail.com

Venkat M Shinde

Department of Botany, Gulbarga University, Kalaburagi, Karnataka, India
Email: vmshinde0690@gmail.com

Laishram Shantikumar Singh

Department of Microbiology, Faculty of Science, Assam downtown University, Guwahati, Assam, India, Email: skllaishram@gmail.com

Abstract:

Silver nanoparticles (Ag NPs) have applications in electrochemistry, energy, bioanalysis, and even environmental monitoring. This is particularly true in the field of antibiotic research. The goal of this work was to determine how the addition of polar components altered the physicochemical characteristics of Ag NPs. Throughout triethylene glycol monoethyl ether, silver nanoparticles were dispersed to keep them from adhering to one another and to maintain their stability. The interaction of the NPs with DNA was examined by researchers to gauge the impact of the dispersion on biocompatibility. The DNA-coated Ag NPs may reduce the fluorescence of FAM-DNA. According to research on DNA adsorption and desorption, the order of interaction between DNA functional groups is phosphate > T > C > A > G. We were able to more thoroughly assess the effectiveness of the antibacterial coating on the Ag NPs by employing marine pathogenic bacteria. Because of the polar component, Ag NPs' antibacterial activity has slightly decreased. By interacting with Ag NPs, small molecules like bases may catalyze the creation of the antimicrobial chemical Ag⁺. Ag NP may be able to use the findings in some way.

Keywords: Silver nanoparticles (Ag NPs), antibacterial activity, green synthesis.

1. Introduction

Due to their amazing properties, silver nanoparticles (Ag NPs) [1] are of great interest to many individuals. Silver is employed in printable inks and printed conductors due to its strong conductivity and resilience to oxidation. Wide-ranging antibacterial activity is exhibited by inorganic silver nanoparticles (NPs) [2]. As demonstrated by Salem and colleagues [3], the intestinal disorder-causing bacteria *Escherichia coli* and *Vibrio cholerae* cannot stand a chance against the Ag NPs. Panák and colleagues discovered that 0.05 mg/L of Ag NPs was enough to stop the growth of *Candida spp.*, but that it had little to no impact on the proliferation of human fibroblasts [4]. Ag NPs prevent virus-host cell adhesion, as demonstrated in experiments by the Elechiguerra team [5]. [6, Ag NPs impede the growth of both Gram-positive and Gram-negative bacteria] was the finding of researchers lead by Gurunathan. Some antibiotic-resistant bacteria developed as a result of increased usage, however the majority of these strains lacked Ag NP resistance. Ag NPs' antibacterial qualities have made them widely used in a number of items, including textiles [13, 14], medical devices [9-11], food packaging [12], air purifiers [15], and wound dressings [7, 8].

Ag NPs are highly biocompatible and can self-assemble with nucleic acids, proteins, and carbohydrates. The melting point of the stem duplex must be raised in order to liberate Dox. HepG-2 cells are made much more vulnerable to chemotherapy by specific DNA sequences [18]. A growing number of applications for silver nanoparticles (Ag NPs), including drug delivery, biosensors, and disease diagnosis, are being explored. Modern antibacterial technology and a vast range of efficient antibacterial chemicals are the products of years of devoted research. Copper (Cu) may exert alloy properties including corrosion and wear resistance, as Zhang and his team showed, indicating it might be used in biomedical materials due to its potent biological and antibacterial effect. There isn't enough copper, though, and too much of it can be harmful to people.

Zhang and his team improved the atomic nickel-titanium alloy's antibacterial capabilities by adding copper to it [26]. Using computer-simulated click chemistry, the Huang-led team created a paste xerogel that serves as a portable antibiotic for bacterial wounds. 60% of the time, gel made of sulfuric acid and static electricity are effective against staphylococcus aureus infections [27]. Unlike silver nanoparticles, which have a wide range of possible applications, this was only beneficial for treating serious disorders. The advancement of antimicrobial tactics including photothermal spectroscopy, photocatalytic antibacterial technology, and others has occurred concurrently with the advancement of optical technology.

The interaction between the shell and the core of a bimetallic organic framework became the focus of the work by Luo et al. It is possible that porphyrin, by increasing the transit of electrons stimulated by PB light, can increase photocatalytic activity. Light at a wavelength of 660 nm generates large amounts of singlet oxygen, which has an antimicrobial impact [28]. Zinc ions were incorporated into a hybrid nanosheet developed by Li's team and given the name (g-C₃N₄-Zn²⁺@GO (SCNZn²⁺@ GO). Rapid exposure to light (660 nm and 808 nm) for wound sterilization and treatment [29] was achieved by electrostatic bonding and stacking interaction. One putative mechanism by which 808nm light affects bacterial metabolism is by

the induction of high temperatures. Active oxygen generated under 660 nm light may also have an antibacterial impact by interfering with bacterial metabolism and protein folding.

The numerous benefits of silver nanoparticles include their intense sterilizing power, antibacterial capabilities, ease of production, minimal environmental impact, and resistance to medication resistance. It became a common ingredient in many products due to its antibacterial properties. Injuring bacteria with nanosilver changed their habitat, harmed their cell walls, and damaged their DNA, among other ways. The silver nanoparticle antibacterial procedure was challenging and affected by a number of factors. According to Hu et al.'s research, DNA might be able to scrape Ag NPs, releasing Ag⁺. Additionally, it was demonstrated that cytosine had the best etching performance [30]. Actually, the major ion that killed the bacterium was Ag⁺. Ag NPs are, however, unstable and prone to aggregation. Ag NPs would absorb various polar molecules when exposed to the environment because of their positively charged surface. This necessitates research into the characteristics of Ag NPs coated with polar substances.

Ag NPs function *in vivo* as antibacterial agents by interacting with polar macromolecules. Investigations are being done into how polar coats affect the properties of Ag NPs. In this study, we examined the properties of Ag NPs coated with various polar substances. We choose Ag NPs that have been dissolved in triethylene glycol monoethyl ether, a commercially available solvent. We were curious about the strange characteristics of the Ag NPs and what impact they would have. Given that DNA may etch Ag NPs, we examined how this interaction influenced the antibacterial activity of the Ag NPs.

2. Resources and Techniques

2.1. Substances. The adenine, guanine, cytosine, and thymine were all provided by Sigma-Aldrich, as were the Ag NPs (50nm). We ordered purified and desalted oligonucleotide sequences from Shanghai Sangon Biotech. Each DNA sequence was also identified by its fluorescence. Glucose, fructose, and silver nitrate (AgNO₃) were all supplied by Sinopharm Group for use in the analysis. We ordered polystyrene plates with 96 wells from Corning, Inc. The experiment was conducted with ultra-high purity water (18.0M). In our experiment, silver nanoparticles were pre-coated with triethylene glycol monoethyl ether.

2.2 Ag NPs' characterization,

2.2.1. Section Transmission electron microscopy After drying the particle dispersions on a holey carbon copper grid, TEM (Philips CM 10) was used to examine the morphology of the Ag NPs.

2.2.2 Infrared Fourier transforms spectrometer The potassium bromide solution, the nanosilver-DNA conjugate solution, and the dried Ag NPs were stored separately. The sample was prepared with somewhat more than 300 mg of potassium bromide. The samples were capillary-tube-selected, then ground. Later, a pill was made through pressing; FT-IR spectroscopy was used to analyze the spectrum.

2.2.3 Dynamic light scattering A Zetasizer Nano particle size analyzer (Malvern, London, UK) was used to measure the dimensions of the Ag NPs and to assess their potential surface area. To dilute the Ag NPs, 2 ml of sterile water was used. From each of these samples, a 3mL detection sample was taken. A concentration of 0.2 mM AgNPs was found in the potential.

2.2.4 X-Ray Diffraction Analysis. Powder X-ray diffraction (XRD) patterns were obtained using a Bruker D8 diffractometer (Bruker, Germany) and Cu K radiation from a variety of

samples. The pattern was recorded in 0.05° increments, with 1 second spent counting for each step across the whole range of $5-90^\circ$.

2.3 AgNPs and DNA interaction Fluorescently labeled DNA measuring 100 m in length was produced and kept in ultrapure water for future use. The four 6-carboxyfluorescein-labeled DNA strands (designated FAM-A15, FAM-T15, FAM-C15, and FAM-G15) were employed in the studies.

Initial DNA samples were deposited in a 96-well plate at a concentration of 10nM. The fluorescence signal was then tracked for 3 minutes while the multiplate reader was in kinetic mode. The Ag NPs' DNA contact was recorded using a versatile microplate reader called the M2000 (Tecan, Switzerland). The wavelengths of 485 nm for excitation and 525 nm for emission were used.

A significant initial value for the fluorescence signal was determined. After giving 1 mM Ag NPs, we monitored the situation for 12 minutes. We also studied how various functional groups on DNA impacted Ag NPs' ability to bind to DNA. The experiment's components were examined with competitive adsorption tests. For 15 minutes, we let the assays remain at room temperature after adding the FAM-24mer sequence and the Ag NPs solution and mixing thoroughly. Substitutes for the DNA's functional groups were introduced, including phosphate buffer, the four nucleotide bases, glucose, and fructose. The microplate reader was successful in capturing the fluorescence signal.

2.4 Ag NPs' Inhibitory Activity on Sea Pathogenic Bacteria To see if the Ag NPs affected the growth of the marine bacteria *V. anguillarum* and *Edwardsiella tarda*, the Oxford cup and spread-plate method was used. After inoculating LB medium with the bacterial strains, they were grown for 16 hours at 30°C and 180 rpm. The seed solution was made by serially diluting the bacterial active solution to a concentration of 10^{-3} . Then, the seed solution was diluted to 100 L and spread on LB agar plates. A volume of 150 L was added as a test to the Oxford cups. The same amount of 75% ethanol was employed concurrently as a positive control.

After that, the plates went into the incubator and stayed there for 24 hours at 30 degrees Celsius. A 600 nm spectrophotometer reading revealed the presence of the broth.

3. Findings and Analysis

3.1 Ag NPs are characterised in section. Based on dynamic light scattering (DLS) measurements, the average size of the Ag NPs is 457 nm. As can be seen in Figure 1(a), silver nanoparticles typically took on a spherical shape. The range of allowable particle size distribution variability is small. The results showed that the diluted Ag NP solution performed just as well as the pure solution. Figure 1(b) clearly demonstrates the positive charge of Ag NPs in ultrapure water. Silver nanoparticles have a zeta potential of -13.7 mV. It was hypothesized that the polar dispersion had been deposited on the Ag NPs since the triethylene glycol monoethyl ether dispersant showed a modest negative charge after being diluted with ultrapure water.

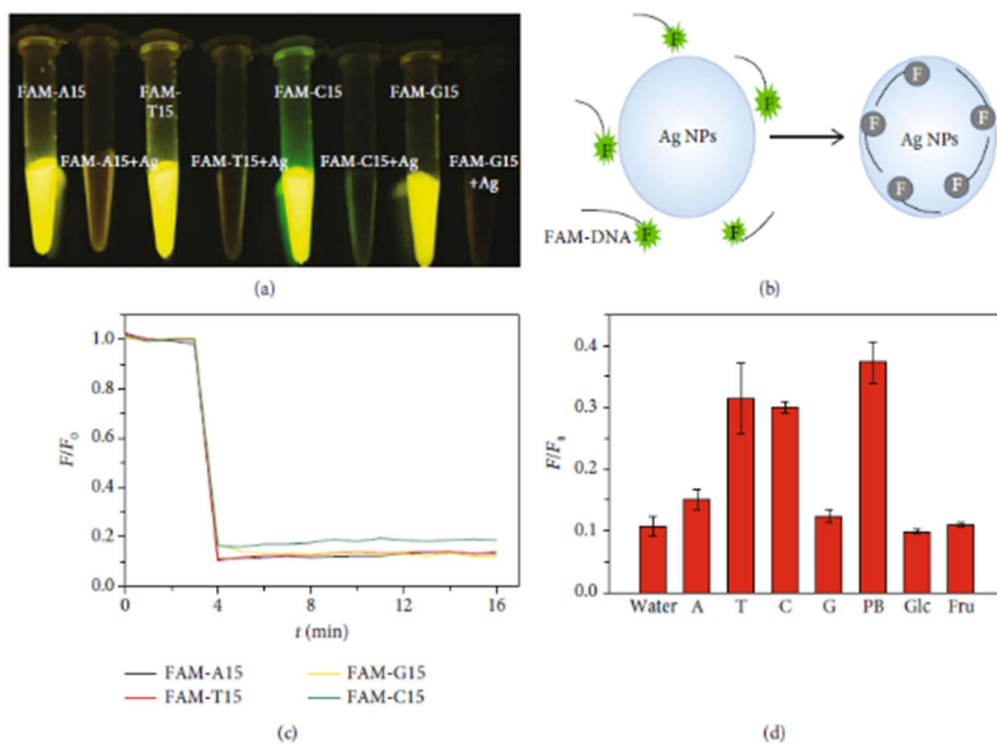


Fig – 1: Dynamic light scattering (DLS) measurements

3.2. AgNPs and DNA interaction The fluorescence signal was dampened and an electron transfer occurred when Ag NPs interacted with FAM-DNA, as illustrated in Figure 2(a). As can be seen in Figure 2(b), the fluorescence of the DNA was reduced when it was mixed with Ag NPs after being labeled with FAM. The fast decrease in fluorescence intensity shown in the fluorescence kinetic spectra (Figure 1(c)) of FAM-DNA-labeled Ag NPs demonstrates that the two particles came into contact extremely quickly. According to the results, the four distinct FAM-A15, FAM-T15, FAM-C15, and FAM-G15 oligonucleotide sequences were all predicted to be compatible with Ag NPs.

DNA is a large molecular molecule, and deoxyribonucleotides are its building blocks. Deoxyribonucleotides are made up of the sugar deoxyribose, the bases adenine, thymine, cytosine, and guanine, and the phosphate group (P3) that holds them all together.

Analogues of functional groups were studied to see how they affected DNA-Ag NP interactions. They intentionally sought out mirror images. For the phosphate backbone, fructose and glucose were substituted for ribose and the inorganic phosphate buffer solution. The FAM-24mer makes use of its nucleotides in an entirely arbitrary order. Gold, argon, carbon, and thorium were the next strongest ions after phosphate. Figure 2(d) displays the effect of the phosphate buffer solution and four distinct nucleotide bases on the interaction. The contact process is barely affected by either fructose or glucose. The capacity of Ag NPs to interact with DNA may be relatively unaffected by the presence of deoxyribose. Adenine and guanine have a lower affinity for Ag NPs than thymine and cytosine, with the phosphate backbone likely playing a role.

Figure 2 depicts the fluorescence lifetime of labeled DNA and Ag NPs together. A rapid drop in fluorescence lifetime was seen in all parts of the sample, making it clear that Ag NPs and DNA were mixing [32]. The Ag NPs isolated from the four different bases were likewise separated using TEM. The capacity of Ag NPs to self-assemble is improved by the adsorption of FAM-C15, and then FAM-A15 (Figure 1). The research showed that DNA might change the surface charge of silver nanoparticles. Ag NPs were observed to rapidly cluster after interacting with DNA in our experiments. In EP tubes, condensation formed. The same thing happened in the investigation of Zhang et al. [33] when they exposed Au NPs to thiolate DNA. The binding of Ag NP to DNA relies heavily on the phosphate backbone. It's possible that Ag NPs will form a chemical coordination bond with the phosphates in DNA. The surface of Ag NPs is positively charged, while the phosphate backbone is negatively charged.

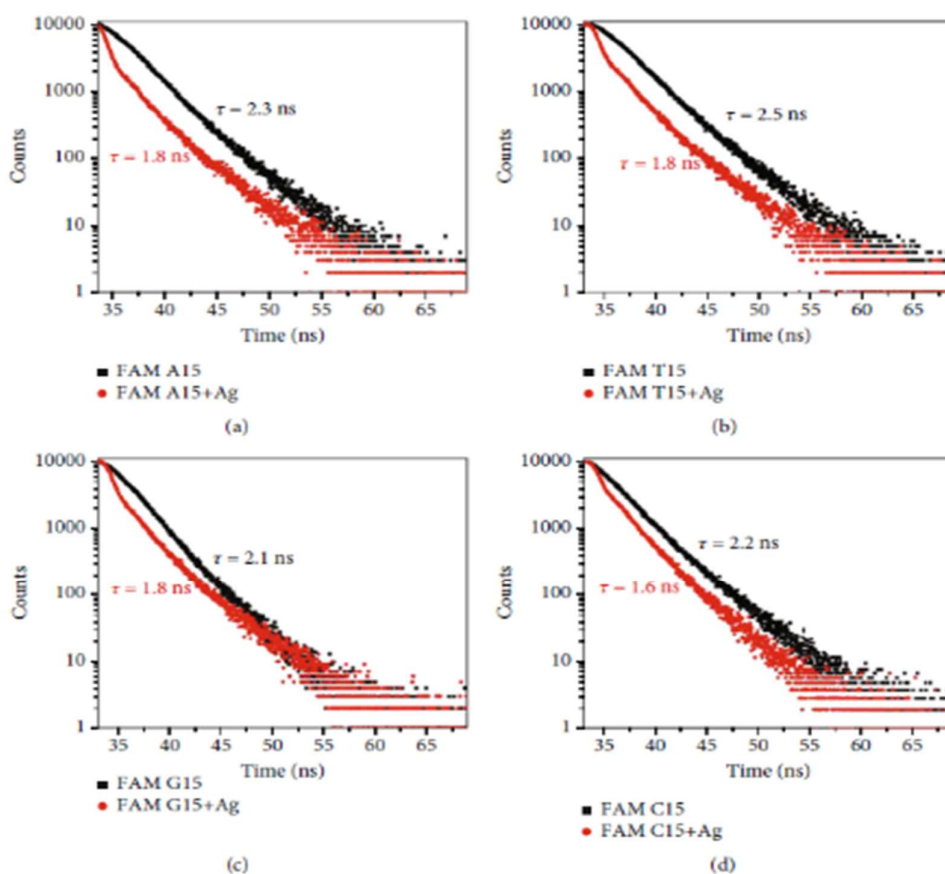


Figure:2 AgNPs and DNA interaction

As a result, they feel an intense electric pull toward one another. Four distinct nucleic bases aid in adsorption, with thymine being the most crucial. Ribose only slightly influences adsorption. It was previously believed that the base and the Ag NPs would create an N-H hydrogen bond. We eluted DNA that had been adsorbed by Ag NPs from a 1M urea solution to see if this was the case. The absence of any effect from elution was confirmed to be the case. The length of DNA that was absorbed by the Ag NPs surface was not consistent. DNA was seen to be twisted on the Ag NPs (Figure 2).

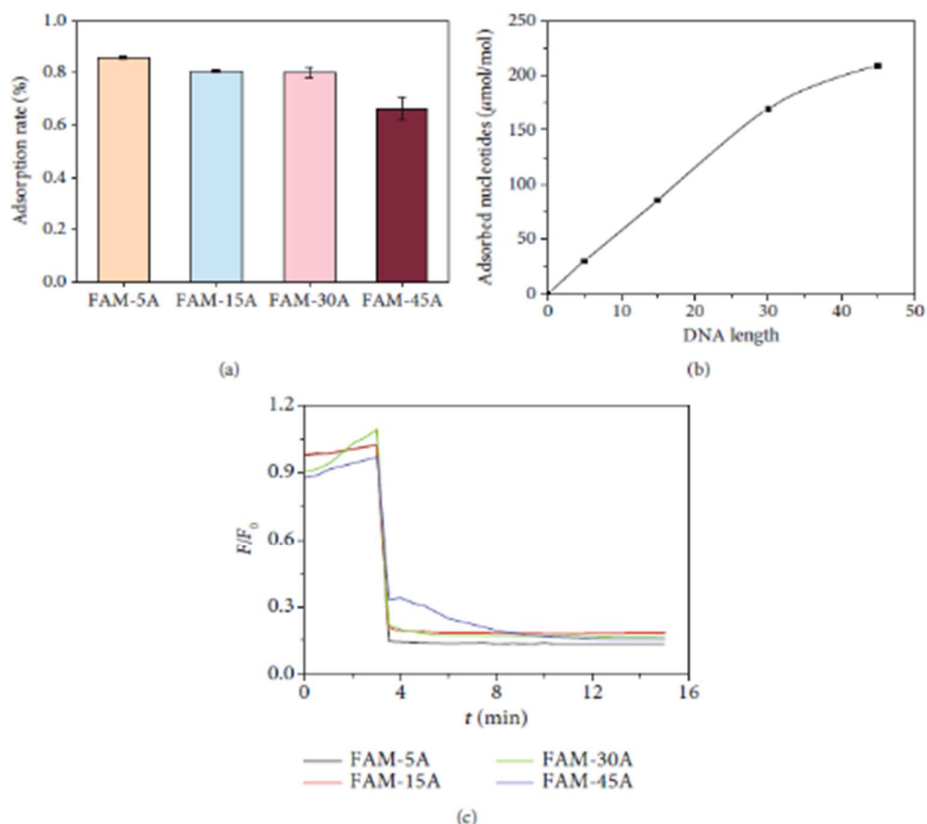


Figure:3 Testing with Ag NPs and each of the four FAMs

Third Part: Desorption of DNA. Once Ag NPs have absorbed fluorescently tagged DNA, DNA desorption can be induced by the addition of an inorganic phosphate buffer and nucleobases. As the concentration of cytosine increased, more degraded DNA was produced. Figure 3 shows the results of testing with Ag NPs and each of the four FAMs (FAM-A15, FAM-T15, FAM-C15, and FAM-G15). FAM-T15 was the most difficult of the four DNA sequences tested to desorb. Ag NPs and FAM-T15 are believed to be the most effective adsorption agents. DNA desorption was stimulated by adding free cytosine (10 M vs. 10 nM) at a concentration almost a thousand times higher than that of FAM-15C. Ag NPs have a powerful interaction with DNA bases. Since physical adsorption is permanent, it was thought that high contact pressures represented this phenomenon symbolically. Desorption investigations employing phosphate buffer, adenine, thymine, and guanine yielded similar results.

3.4. DNA Adsorption Mechanism. The formation of a hydrogen bond between Ag NPs and DNA is demonstrated by comparing the FT-IR spectra (Figure 4(a)). Without infrared absorption peaks, metals cannot transmit even infrared light from metal nanoparticles. The infrared peak typically associated with Ag nanoparticles was thus approximated using triethylene glycol monoethyl ether. DNA and polar solvent peaks were clearly seen in the infrared spectra of Ag NPs and DNA conjugates. This wide band between 3387.01 cm^{-1} and 3422.69 cm^{-1} may have been set off by -OH tensile vibration. C=O had a small absorption peak at 1646.70 cm^{-1} , which was easily discernible. In triethylene glycol monoethyl ether, our model predicts the presence of a C-O electron cloud that overlaps with itself. Absorption peak

appeared at 1398.03 cm^{-1} because of C-H bending vibration. DNA is typically viewed as an organic macromolecule.

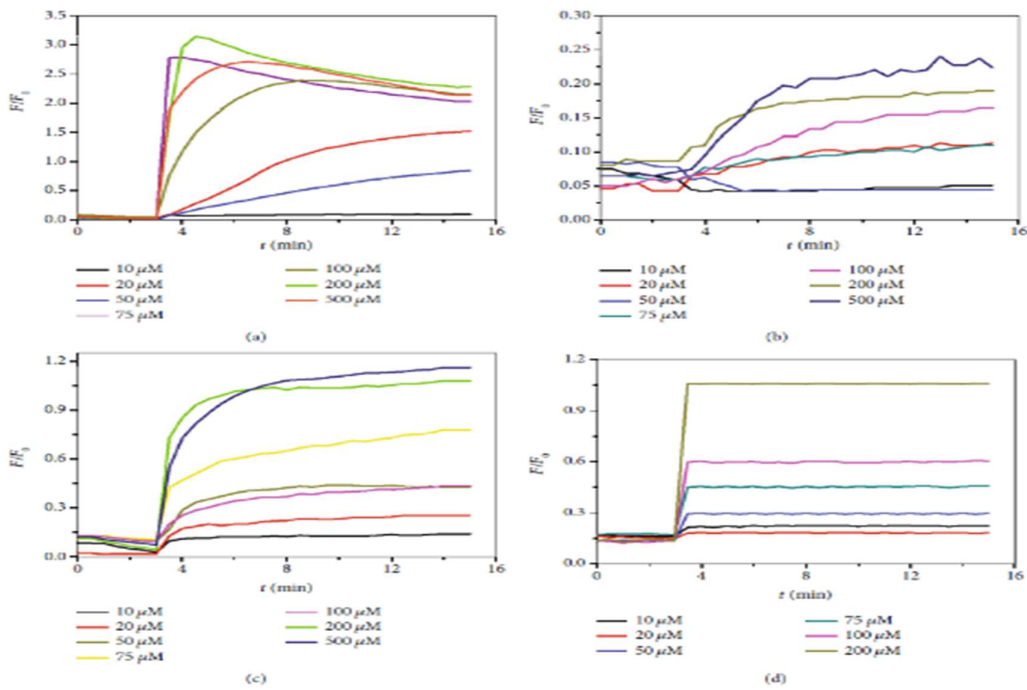
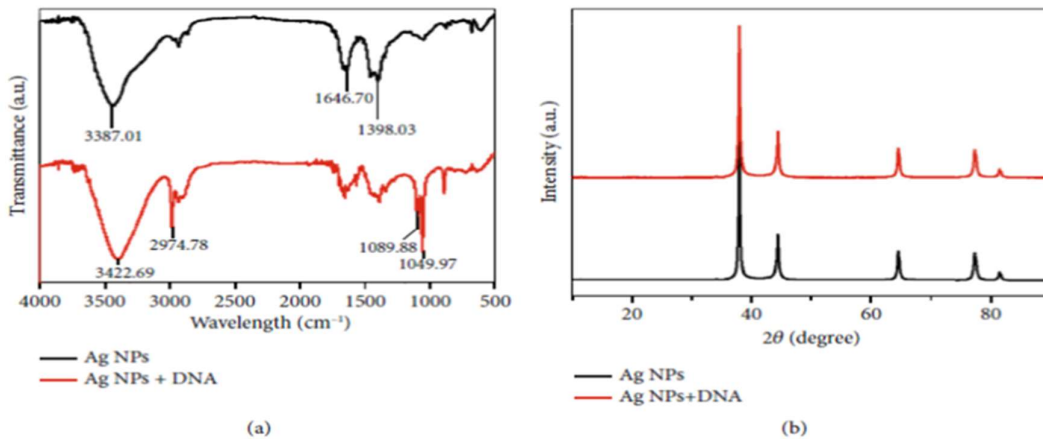


Figure:4 DNA Adsorption Mechanism

Infrared spectra of both Ag NPs and DNA conjugate showed characteristic peaks at 2974.78 cm^{-1} (C-H in $-\text{CH}_2$) and 1089.88 cm^{-1} (C-O bond absorption). C-N bond's signature peak is clearly evident at 1049.97 cm^{-1} . The XRD spectra in Figure 5(b) show that the unique Ag NP peaks existed prior to and after DNA adsorption. The crystal structure of Ag NPs is shown to be unaltered prior to and during DNA adsorption (Figure 5(b)).



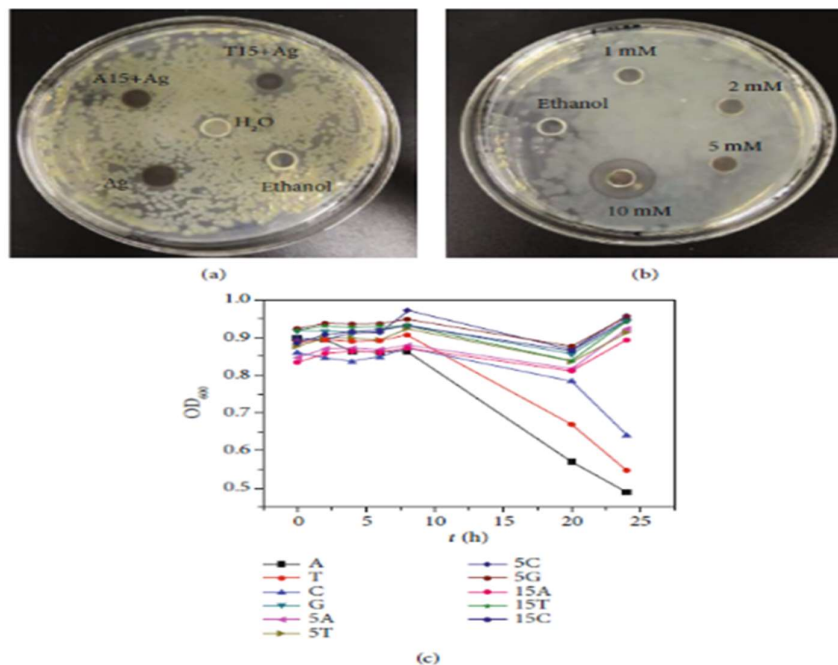


Figure: 5 (a) Infrared spectra 5(b) XRD spectra

3.5 Impact of Antimicrobial Activity In order to examine the effect of polar dispersion on the antibacterial activities of Ag NPs, three marine pathogenic bacteria (*V. anguillarum*, *E. tarda*) were used in the experiment. Bactericidal effects of Ag NPs and Ag NPs-DNA conjugates at 5 mM were tested against *V. anguillarum* using the Oxford cup method. The use of Ag NPs or Ag NPs-DNA did not result in the formation of a distinct inhibitory zone on the plate. Figure 6(b) shows that the antibacterial activity of the Ag NP was already noticeable at a concentration of 10mM. As can be shown in Figure 6(c), the effects of Ag NPs and DNA conjugates on the growth of *E. tarda* are quite similar. In particular, adenine's inclusion in the base-Ag NP formulation had a considerable effect.

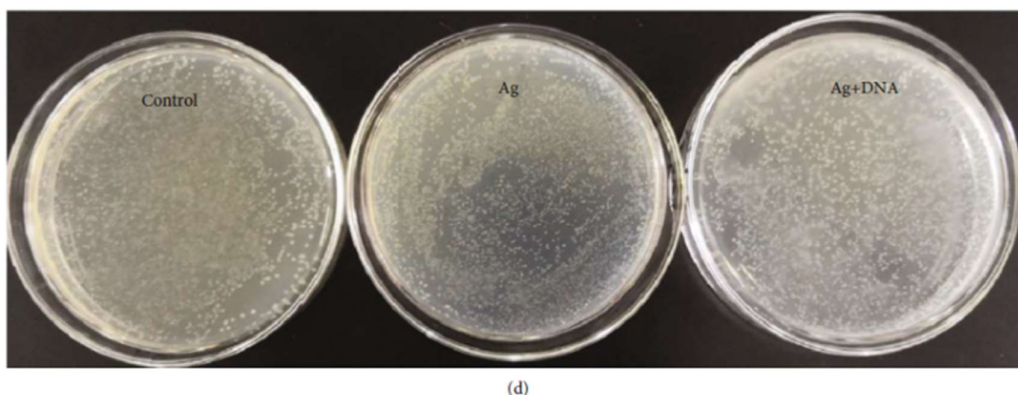


Figure: 6 Impact of Antimicrobial Activity

An A was more valuable than a T or C. There's a suggestion that exposing Ag NPs to bases causes them to release even more silver ions, considerably increasing their antimicrobial potency. Figure 6(d) shows that the use of Ag NPs coated with a polar dispersion in the *E. tarda* dissemination approach has no antibacterial effect. Results from using either pure Ag

NPs or a mixture of pure Ag NPs and DNA were identical to those obtained from the control. The polar dispersant did its job and stopped the Ag⁺ leak.

Some of the factors that affect Ag NPs' sterilising power include their size, shape, surface potential, coating agent, and dispersion. The degree to which Ag NPs are compact influences how effectively they inhibit bacterial growth [34]. Our results showed that when the concentration of triethylene glycol monoethyl ether on Ag nanoparticles increased, the antibacterial activity of the particles almost totally decreased. Polarization diminished the antibacterial activity of Ag NPs. In the process of killing bacteria, Ag NPs are known to release highly biologically active silver ions [22–24, 28–29]. These ions are able to enter the cell wall and cause the bacteria's death. We postulated that dispersants would inhibit the release of silver ions from Ag NPs, therefore diminishing the particles' antibacterial activity.

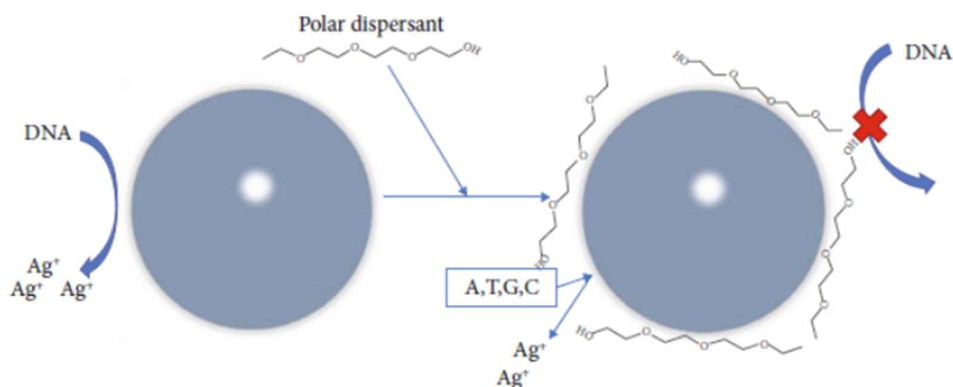


Figure: 7 Complex interaction between Ag NPs and nucleotide bases in DNA

The etch effect of DNA on Ag NPs during interaction with DNA was discovered in 2019 [25] by Zhang's team. As surface silver ions were eliminated, Ag NPs became more resistant to bacteria and cancers [25]. with a comparison with Ag NPs coated with triethylene glycol monoethyl ether, we found that the former was less affected by DNA's etching action, leading us to conclude that the polar dispersion provided this protection. However, the results of our experiments demonstrated that nucleotide bases remained in etching Ag NPs.

In Figure 7, we see a simplified depiction of the complex interaction between Ag NPs and nucleotide bases in DNA. The polar components coated on the Ag NPs, however, have the ability to bind to biomacromolecules, as our research shown. On the other hand, the antibacterial action may be severely weakened.

4. Conclusion

The effect of the polar triethylene glycol monoethyl ether dispersion used to cover the Ag nanoparticles was the study's main area of interest. Ag NPs' interaction with DNA due to adsorption could not be avoided. Ag NPs can still lessen the fluorescence of FAMDNA. The adsorption is significantly influenced by the chemical composition of bases and phosphates.

The following relationships between DNA's functional groups have been discovered through adsorption and desorption studies: phosphate>T>C>A>G. Polar dispersion of Ag NPs hindered their antibacterial activity. The Ag⁺ that Ag NP surfaces produce when they interact with tiny molecules like bases may also be a factor in the antibacterial action of these materials. Ag NPs produce highly physiologically active silver ions, which have an antibacterial effect; however, polar substances have the potential to change this property. Although treating Ag NPs with bases significantly boosted their antibacterial activity, coating them with polar lipids significantly decreased it. The amount of bases in Ag NPs can be changed to alter the degree to which they hinder bacterial growth. The use of silver nanoparticles as a biological, medicinal, and antimicrobial tool is supported theoretically in this paper.

References

- [1] G. R. Tortella, O. Rubilar, N. Durán et al., “Silver nanoparticles: toxicity in model organisms as an overview of its hazard for human health and the environment,” *Journal of Hazardous Materials*, vol. 390, no. 5, p. 121974, 2020.
- [2] A. Feng, J. Cao, J. Wei, F. Chang, Y. Yang, and Z. Xiao, “Facile synthesis of silver nanoparticles with high antibacterial activity,” *Materials*, vol. 11, no. 12, p. 2498, 2018.
- [3] W. Salem, D. R. Leitner, F. G. Zingl et al., “Antibacterial activity of silver and zinc nanoparticles against *Vibrio cholerae* and enterotoxigenic *Escherichia coli*,” *International Journal of Medical Microbiology*, vol. 305, no. 1, pp. 85–95, 2015.
- [4] A. Panáček, M. Kolář, R. Večeřová et al., “Antifungal activity of silver nanoparticles against *Candida* spp,” *Biomaterials*, vol. 30, no. 31, pp. 6333–6340, 2009.
- [5] J. L. Elechiguerra, J. L. Burt, J. R. Morones et al., “Interaction of silver nanoparticles with HIV-1,” *Journal of Nanobiotechnology*, vol. 3, no. 1, p. 6, 2005.
- [6] S. Gurunathan, J. W. Han, D. N. Kwon, and J. H. Kim, “Enhanced antibacterial and anti-biofilm activities of silver nanoparticles against Gram-negative and Gram-positive bacteria,” *Nanoscale Research Letters*, vol. 9, no. 1, p. 373, 2014.
- [7] D. Archana, B. K. Singh, J. Dutta, and P. K. Dutta, “Chitosan- PVP-nano silver oxide wound dressing: in vitro and in vivo evaluation,” *International Journal of Biological Macromolecules*, vol. 73, no. 2, pp. 49–57, 2015.
- [8] H. Agarwal, A. K. Gupta, N. Gupta, S. Mukharjee, and C. K. Durga, “Comparison of results of silver-impregnated dressing with povidone iodine based-dressing in patients with diabetic foot,” *Hellenic Journal of Surgery*, vol. 87, no. 6, pp. 465–467, 2015.
- [9] D. Huo, J. He, H. Li et al., “Fabrication of Au@Ag core-shell NPs as enhanced CT contrast agents with broad antibacterial properties,” *Colloids & Surfaces B Biointerfaces*, vol. 117, no. 5, pp. 29–35, 2014.
- [10] X. Chen and H. J. Schluesener, “Nanosilver: a nanoparticle in medical application,” *Toxicology Letters*, vol. 176, no. 1, pp. 1–12, 2008.
- [11] K. Hosoyama, M. Ahumada, C. D. McTiernan et al., “Multifunctional thermo-crosslinkable collagen-metal nanoparticle composites for tissue regeneration: nanosilver vs. nanogold,” *RSC Advances*, vol. 7, no. 75, pp. 47704–47708, 2017.
- [12] J. C. Hannon, J. P. Kerry, M. Cruz-Romero, S. Azlin-Hasim, and E. Cummins, “An assessment of the migration potential of nanosilver from nanoparticle coated low density polyethylene food packaging into food simulants,” *Food Additives & Contaminants. Part A, Chemistry, Analysis, Control, Exposure & Risk Assessment*, vol. 33, no. 1, pp. 167–178, 2015.

- [13] N. V. K. Thanh and N. T. P. Phong, "Investigation of antibacterial activity of cotton fabric incorporating nano silver colloid," *Journal of Physics: Conference Series*, vol. 187, no. 1, p. 012072, 2009.
- [14] S. H. Jeong, Y. H. Hwang, and S. C. Yi, "Antibacterial properties of padded PP/PE nonwovens incorporating nano-sized silver colloids," *Journal of Materials Science*, vol. 40, no. 20, pp. 5413–5418, 2005.
- [15] Y. W. Yang and J. L. Liu, "Latest advances in the researches in and application of nanoparticle silver," *Industrial Catalysis*, vol. 271, no. 2, pp. 343–350, 2003.
- [16] P. Prasher, M. Sharma, H. Mudila et al., "Emerging trends in clinical implications of bio-conjugated silver nanoparticles in drug delivery," *Colloid and Interface Science Communications*, vol. 35, no. 3, p. 100244, 2020.
- [17] M. Rahimi, E. B. Noruzi, E. Sheykhsaran et al., "Carbohydrate polymer-based silver nanocomposites: recent progress in the antimicrobial wound dressings," *Carbohydrate Polymers*, vol. 231, p. 115696, 2020.
- [18] T. T. Zhao, Q. Y. Chen, and H. Yang, "Spectroscopic study on the formation of DNA-Ag clusters and its application in temperature sensitive vehicles of DOX," *Spectrochimica Acta Part A Molecular & Biomolecular Spectroscopy*, vol. 137, pp. 66–69, 2015.
- [19] J. C. Trefry, J. L. Monahan, K. M. Weaver et al., "Size selection and concentration of silver nanoparticles by tangential flow ultrafiltration for SERS-based biosensors," *Journal of the American Chemical Society*, vol. 132, no. 32, pp. 10970–10972, 2010.
- [20] J. Willem de Vries, S. Schnichels, J. Hurst et al., "DNA nanoparticles for ophthalmic drug delivery," *Biomaterials*, vol. 157, pp. 98–106, 2018.
- [21] Q. Pan, J. Zhang, X. Li et al., "Construction of novel multifunctional luminescent nanoparticles based on DNA bridging and their inhibitory effect on tumor growth," *RSC Advances*, vol. 9, no. 26, pp. 15042–15052, 2019.
- [22] N. Kasyanenko, V. Bakulev, I. Perevyazko et al., "Model system for multifunctional delivery nanoplatforms based on DNAPolymer complexes containing silver nanoparticles and fluorescent dye," *Journal of Biotechnology*, vol. 236, pp. 78–87, 2016.
- [23] X. Xu, J. Wang, F. Yang, K. Jiao, and X. Yang, "Label-free colorimetric detection of small molecules utilizing DNA oligonucleotides and silver nanoparticles," *Small*, vol. 5, no. 23, pp. 2669–2672, 2009.
- [24] J. Fu, Z. Zhang, and G. Li, "Progress on the development of DNA-mediated metal nanomaterials for environmental and biological analysis," *Chinese Chemical Letters*, vol. 30, no. 2, pp. 285–291, 2019.
- [25] E. Zhang, S. Fu, R. X. Wang et al., "Role of Cu element in biomedical metal alloy design," *Rare Metals*, vol. 38, no. 6, pp. 476–494, 2019.
- [26] J. Zhang, Y. H. Sun, Y. Zhao et al., "Antibacterial ability and cytocompatibility of Cu-incorporated Ni–Ti–O nanopores on NiTi alloy," *Rare Metals*, vol. 38, no. 6, pp. 552–560, 2019.
- [27] B. Huang, X. Liu, L. Tan et al., "“Imitative” click chemistry to form a sticking xerogel for the portable therapy of bacteria infected wounds," *Biomaterials Science*, vol. 7, no. 12, pp. 5383–5387, 2019.
- [28] Y. Luo, J. Li, X. Liu et al., "Dual metal–organic framework heterointerface," *ACS Central Science*, vol. 5, no. 9, pp. 1591–1601, 2019.

- [29] Y. Li, X. Liu, L. Tan et al., “Rapid sterilization and accelerated wound healing using Zn²⁺ and graphene oxide modified g-C₃N₄ under dual light irradiation,” *Advanced Functional Materials*, vol. 28, no. 30, pp. 1800299.1–1800299.12, 2018.
- [30] S. Hu, T. Yi, Z. Huang et al., “Etching silver nanoparticles using DNA,” *Materials Horizons*, vol. 6, no. 1, pp. 155–159, 2019.
- [31] V. K. Sharma, K. M. Siskova, R. Zboril, and J. L. Gardea-Torresdey, “Organic-coated silver nanoparticles in biological and environmental conditions: fate, stability and toxicity,” *Advances in Colloid and Interface Science*, vol. 204, pp. 15–34, 2014.
- [32] A. Ghosh, N. Karedla, J. C. Thiele, I. Gregor, and J. Enderlein, “Fluorescence lifetime correlation spectroscopy: basics and applications,” *Methods*, vol. 140-141, pp. 32–39, 2018.
- [33] X. Zhang, M. R. Servos, and J. Liu, “Fast pH-assisted functionalization of silver nanoparticles with monothiolated DNA,” *Chemical Communications*, vol. 48, no. 81, pp. 10114–10116, 2012.
- [34] M. Guzman, J. Dille, and S. Godet, “Synthesis and antibacterial activity of silver nanoparticles against gram-positive and gram-negative bacteria,” *Nanomedicine: Nanotechnology, Biology and Medicine*, vol. 8, no. 1, pp. 37–45, 2012